www.czasopisma.pan.pl PAN www.journals.pan.pl

ARCHIVES of FOUNDRY ENGINEERING

ISSN (2299-2944)
Volume 21
Issue 1/2021

137 – 145

10.24425/afe.2021.136090

20/1

Published quarterly as the organ of the Foundry Commission of the Polish Academy of Sciences

Effect of High-tin Bronze Composition on Physical, Mechanical, and Acoustic Properties of Gamelan Materials

S. Slamet[a, b, *], S. Suyitno[a], I. Kusumaningtyas[a], I.M. Miasa[a]
[a] Universitas Gadjah Mada, Yogyakarta, Indonesia
[b] Universitas Muria Kudus, Kudus, Indonesia
* Corresponding author. E-mail address: sugeng.slamet@umk.ac.id

Received 29.07.2020; accepted in revised form 23.02.2021

Abstract

High tin bronze alloy (Cu>17wt.%Sn) is commonly as raw material to fabricate musical instruments. Gamelan musical instruments in Indonesia are produced using tin bronze alloy raw materials. The tin bronze alloy used by each gamelan craftsman has a different tin composition, generally in the range of Cu(20-24) wt.% Sn. This study aims to investigate the effect of microstructure, density, and mechanical properties of Cu(20-24)wt.%Sn against the acoustic properties processed by the sand casting method.
The material is melted in a crucible furnace until it reaches a pouring temperature of 1100ºC by the sand casting method. The specimens were subjected to microstructure observations, density and porosity as well as mechanical properties testing including tensile strength, bending strength, hardness, and modulus of elasticity. Mechanical properties data then used to calculate several parameters of acoustic properties including speed of sound (c), impedance (z) and radiation coefficient (R). Processes simulation using Finite Element Analysis (FEA) and Experiment Method Analysis (EMA) were carried out to determine acoustic properties including sound intensity, natural frequency and damping capacity.
The experimental result shows that the increase in tin composition in Cu(20-24) wt.% Sn changed the microstructure of coarse grains into dendrite-columned fine grains. Physical properties of density decrease, while porosity increases. Mechanical properties including tensile strength, modulus of elasticity, and bending strength decreased, while the hardness of the alloy increases. The calculation of acoustic parameters such as the speed of sound (c), impedance (z) and radiation coefficient (R) has decreased. Moreover, sound intensity (dB), natural frequency (Hz) and damping capacity also decrease with increasing tin composition. Hence, tin bronze alloy Cu20wt.%Sn is the recommended raw material for the manufacture of gamelan instruments through the sand casting method.

Keywords: Tin bronzes, Mechanical properties, Acoustic properties, Gamelan, Sand casting

1. Introduction

Gamelan is one of the traditional musical instruments in Indonesia, mainly found in Central Java, West Java, and Bali [1,2]. Gamelan is used for instrumental performances that can be performed outdoors or indoors. Gamelan performances played indoors have a better acoustic quality than outdoors [3]. Gamelan is produced using metal through the forging method. Based on the source of the sound produced, a gamelan instrument is an idiophone musical instrument. Gamelan is one of Indonesia's traditional musical instruments that is continually preserved.

High tin bronze alloy (18-25)wt.% Sn is widely used to produce gamelan than brass and cast iron [4–6]. The composition of the high tin bronze alloy utilized as a gamelan material varies from Cu(22-23)wt.%Sn [4], Cu(20-23) wt.%Sn[5], Cu(20-

22.5)wt.% Sn [7], and Cu(20-25) wt.% Sn [6]. The high tin bronze alloy was selected as a musical instrument because it has excellent acoustic properties [4,5,8]. The tin bronze alloy molten metal composition (20-24)wt.%Sn can flow and fill sand molds in thin cavities between 2-3 mm with increasing pouring temperature [9]. However, high tin bronze alloys tend to crack easily when hammered and cannot withstand low temperatures [10]. At temperatures below -20ºC to -25ºC, tin bronze is very brittle and easily cracked, which affects the sound quality of the gamelan. The tin composition in the bronzed alloy used for gamelan craftsmen is diverse due to limited literature toward its effect on physical, mechanical, and acoustic properties.

Gamelan instruments are produced through repeated forging processes to obtain the desired shape and size. To fabricate gamelan via the forging method requires a long time, high production costs, and high energy consumption. To produce a set of gamelan instruments requires a working load of 6-10 persons in 3-4 months. The forging method followed by rapid cooling is the method used to produce a *gong* instrument [4]. The advantage of the forging method is that it can increase density and reduce porosity. However, the forging method produces non-uniform compaction, a relatively rough surface due to oxidation, and the formation of residual stresses which can damage the sound quality and cause cracks in the gamelan [6,7].

The casting method can be an alternative option to produce gamelan. The casting method was chosen because it can produce metal components with complex shapes and is suitable for mass products at a relatively low cost. Some casting methods, such as centrifugal casting are capable of improving mechanical properties [11]. More than 80% of metal components are produced by casting [12]. The sand casting method was selected due it needs viable technology and low production costs.

Flowability and filling ability of the mold cavity are fluidity parameters in the application of the casting method. The fluidity of the metal fluid in the mold cavity is impacted by the increasing alloy composition and the mold media. The low fluidity of metal fluids defects casting products and worsen mechanical properties. The mechanical properties affect the acoustic properties of a musical instrument. Mechanical properties in the form of modulus of elasticity and physical properties in the form of density can be used to predict the high and low frequency and damping capacity [13]. Metallic materials with low stiffness and low modulus of elasticity tend to have lower natural frequencies compared to materials with high stiffness and high modulus of elasticity [14].

The objective of this study is to determine the effect of tin composition on the physical, mechanical, and acoustic properties of tin bronze alloy as raw material for gamelan instruments via the sand casting method. Gamelan instruments via the sand casting method are shown in Figure 1.

Fig.1. Gamelan by sand casting method

2. Materials and method

2.1. Materials for the experiment

The alloy material (Cu = 99.9%, Sn = 99.9%) was melted in the crucible furnace. The tin bronze alloys were varied by Cu(20-24)wt.%Sn then heated up to 1100°C by sand casting method. The materials composition analyzed by spectrometry is shown in Table 1.

The mold using silica oxide sand (SiO_2) is characterized by SEM-EDS depicted in Figure 2. The sand grains are homogenized using a 100 mesh filter. Silica (Si) and oxide (O_2) compounds show a large amount compared to other elements in small amounts e.g Mg, Fe, Na, and Ca. Silica and Oxide compounds form Silica Oxide (SiO_2) which is a ceramic material i.g refractory material.

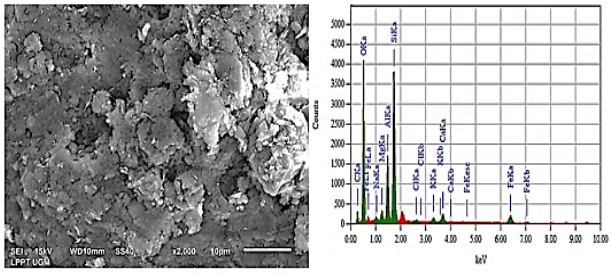

(a) (b)

Fig. 2. SEM-EDS the mold material (a) fractography (b) EDS

The equipment dimension to make the sand mold shown in Figure 3, has a length of 400 mm, a width of 10 mm, and a variation of the mold cavity from 1.5 to 5 mm.

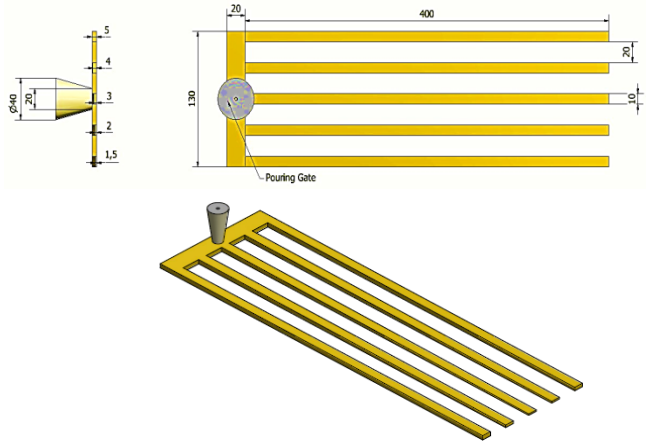

Fig. 3. Mold pattern design

Table 1.
Materials composition

Alloys	Composition (%)						
	Cu	Sn	Zn	Pb	Fe	Ni	Al
Cu20wt.%Sn	79.77	20.06	0.08	0.02	0.04	0.00	<0.001
Cu22wt.%Sn	78.16	21.39	0.03	0.14	0.13	0.10	<0.001
Cu24wt.%Sn	75.13	23.86	0.14	0.20	0.48	0.14	<0.001

2.2. Microstructure characterization

Microstructures were observed using an optical light microscope (Olympus, Japan) with 100X magnification. Casting products 400 x 10 x 5 mm are segmented into specimens 10 x 10 x 5 mm. The specimens were mounted using a mixture of polyester resin and hardener. Polishing used sandpaper with grades 1000 and 1500. Specimens were etched in a mixture of HNO_3: H_2O (50%: 50%) for 5 seconds, then microstructure was observed.

2.3. Density and porosity calculations

Density and porosity were measured using rod-shaped specimens 70 x 10 x 5 mm. The density and porosity of the tin bronze alloy were calculated using the Archimedes formula, where the actual density (g.cm^{-3}) is the ratio between the weight of the specimen in air divided by the difference in value between the weight of the specimen in air and the weight of the specimen in water (g) multiplied by the density of water (g.cm^{-3}). The porosity of specimens (%) is calculated from the ratio between actual density (g.cm^{-3}) and theoretical density (g.m^{-3}). The density and porosity have been calculated using Equations (1) and (2), [15].

$$\rho_b = \frac{w_{air}}{w_{air} - w_{water}} x\ \rho_{water} \quad (1)$$

$$\text{Porosity (\%)} = (1 - \frac{\rho_b}{\rho_{theory}}) \text{ x } 100\% \quad (2)$$

Where ρ_b is actual density (g.cm^{-3}), w_{air} mass in the air (g), w_{water} mass in water (g), ρ_{water} pure water density (1 g.cm^{-3}), and ρ_{theory} the theoretical density of high tin bronze 8.900 g.cm^{-3}.

2.4. Hardness and mechanical properties

Microhardness was measured using the Vickers method with a load is 1 N and holding time is 5 seconds. Tensile test specimens are produced according to ASTM E-8 and ASTM E-290 standards for bending tests with a load of 2000 kg. Tensile testing aims to obtain the Ultimate Tensile Strength (N.mm^{-2}) and modulus of elasticity (N.mm^{-2}) in high tin bronze specimens. A tensile test was conducted using Shimadzu servopulser type EHF-EB 20-40L. The bending test applied at the three-point bending method operated using the universal testing machine (Torsee Universal Testing Machine, Tokyo Testing Machine Mfg.Co., Ltd., Japan) [16]. The gap between each supports was set at 40 mm. A concentrated load F (kg) was given midpoint in between the support. The observed loading force and deflection were recorded for every 0.25 mm of deflection. The bending test (σ_b) and modulus of elasticity (E_b) are calculated using Equations (3) and (4).

$$\sigma_b = \frac{3PL}{2bd^2} \quad (3)$$

$$E_b = \frac{1}{4}\ x\ \frac{L^3}{bh^3} x\ \frac{P}{\delta} \quad (4)$$

where P is the force in the proportional region (N), L the distance between support (mm), δ deflection at the mid-point of the specimen for the given force (mm), and b and h the width (mm) and thickness (mm).

2.5. Finite Element Analysis/FEA

The Finite Element Analysis was simulated using Abaqus software version 6.14. It is proposed to determine the change in displacement and natural frequency. The input variables are the density, modulus of elasticity, and Poisson's ratio (υ = 0.3) for each alloy composition. This FEA specimen is in the form of a rod with dimensions of 125 mm x 10 mm x 5 mm with 0.5 mesh (ASTM E 1876-01) shown in Figure 4.

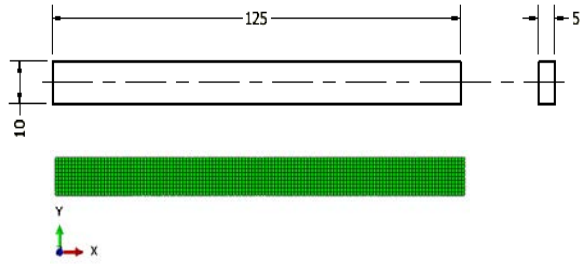

Fig. 4. ASTM E1876-01 (scale: mm)

2.6 Experimental Method Analysis/EMA

The acoustic properties parameters include the speed of sound c (m.s^{-1}), the impedance factor z (kg.m^{-2}.s^{-1}), and the radiation

coefficient R ($m^4 \cdot kg^{-1} \cdot s^{-1}$)[13], calculated by Equations (5), (6) and (7). The acoustic properties are mainly influenced by the modulus of elasticity E ($N.mm^{-2}$) and density ρ ($kg.m^{-3}$) of the material. The Experimental Method Analysis/EMA was carried out by hanging the sample with an elastic rope at a distance of 25 mm from both ends of the test object shown in Figure 5(b). The sample was struck on the surface using a steel hammer. The sound produced by the sample was recorded using Audacity software version 2.1.2. The experimental method analysis was repeated five times regarding frequency (Hz), sound intensity (dB), and damping capacity. Acoustic testing using the experimental method analysis is shown in Figure 5.

$$c = \sqrt{\frac{E}{\rho}} \tag{5}$$

$$z = c.\rho \tag{6}$$

$$R = \frac{c}{\rho} = \sqrt{\frac{E}{\rho^3}} \tag{7}$$

Where; c is the speed of sound ($m.s^{-1}$); E Youngs' modulus ($kg.m^{-2}$); ρ density ($kg.m^{-3}$); z is the impedance ($kg.m^{-2}.det^{-1}$) and R is the radiation coefficient ($m^4.kg^{-1}.det^{-1}$).

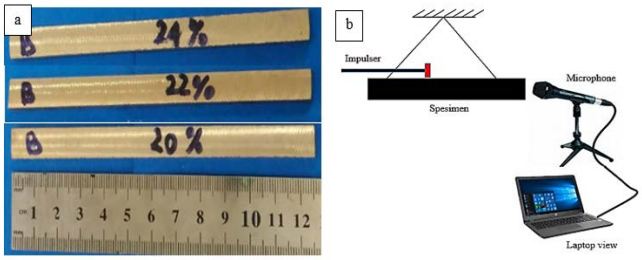

Fig. 5. (a) EMA specimens Cu(20-24)wt.%Sn (b) EMA method for acoustic properties tests.

3. Results and Discussion

3.1 Microstructure

Microstructure analysis of Cu (20-24) wt.% Sn reveals that the increase in tin composition causes the change of coarse grains to the fine grain of columnar dendrites as shown in Figure 6. The growth of the columnar dendrite microstructure is triggered by a decrease in the rate of solidification. Increasing the composition of Sn prolongs the distance between the liquid phase (L) to the liquid-solid phase (α + L). This can be seen in the CuSn binary phase diagram shown in Figure 7(a) and Figure 7(b) showing the gap between the pouring temperature of 1100°C in the liquid phase (L) to the liquid-solid phase (α+ L). The pouring temperature of 1100°C is the superheated temperature that lies above the liquidus line. The decrease in the solidification rate causes phase change from the liquid to the solid lasting longer [17]. Increasing the composition of tin increases the solidification time changing the microstructure of coarse grains to fine granules of columnar dendrites and increases the diffusion of particles in the alloy metal [18]. The decrease in the solidification rate causes a large number of α phase particles to diffuse into the α + δ phase.

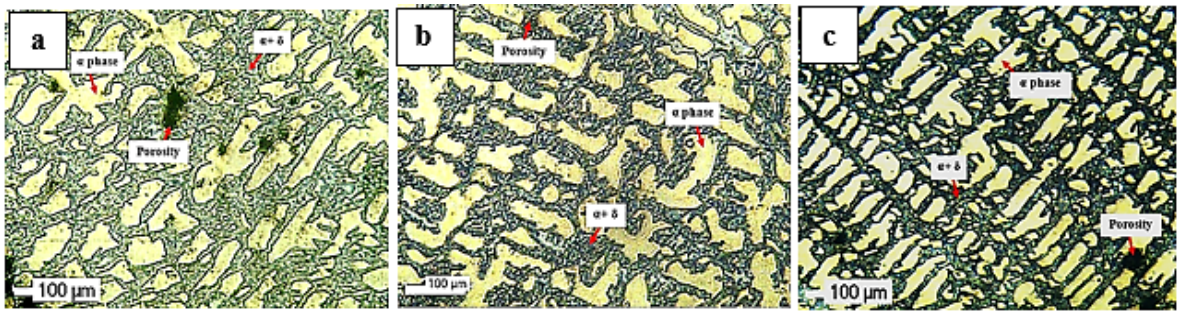

Fig. 6. Microstructure (a) Cu20wt.%Sn (b) Cu22wt.%Sn (c) Cu24wt.%Sn

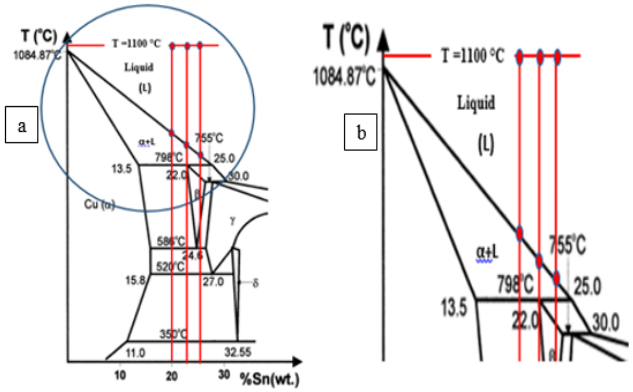

Fig. 7 (a) The tin composition and the pouring temperature are reviewed in the CuSn phase diagram (b) The distance of pouring temperature 1100 ° C to the α + L phase of Cu(20-24)wt.%Sn

3.2. Density and porosity

The percentage of porosity formed in the cast product affects the density. The higher the porosity formed the lower the density. The porosity formed in casting processes is caused by shrinkage of the metal and gas trapped in the molten metal [19]. The sand casting method uses water as a binder between sand particles. Water contains many oxygen compounds as a component of air [20]. Water compounds that break down into air components cause the air content in the mold to increase. The air trapped in the molten metal causes porosity. Figure 6 shows the porosity of the holes caused by trapped air. Apart from the trapped air in the mold, the sand casting method has a large temperature gradient between the mold wall temperature and the poured liquid metal temperature. Metal shrinkage occurs due to temperature differences which increases the cooling rate. The high-bronze tin alloy has a density between 8600 and 8900 kg.m^{-3} [21].

Porosity in cast products is inevitable yet can be minimized by improving the pouring gate and feeding system [19,22]. The viscosity of the liquid metal decreases with increasing pouring temperature and tin composition (20-24)wt% Sn. The low viscosity of the liquid metal causes turbulence when the liquid metal is poured into the mold. The large flow turbulence allows any air bubbles to be trapped in the liquid. Once a high amount of air is trapped in the liquid, it leads to increase porosity thus density decreases. The porosity of tin bronze alloy formed using the sand casting method is highly induced by trapped air. The density decreases from 8842.13 kg.m^{-3} to 8822.98 kg.m^{-3} with increasing Sn content, while porosity increases from 0.650% to 0.865%. The density and porosity of Cu (20-24) wt.% Sn are shown in Figure 8.

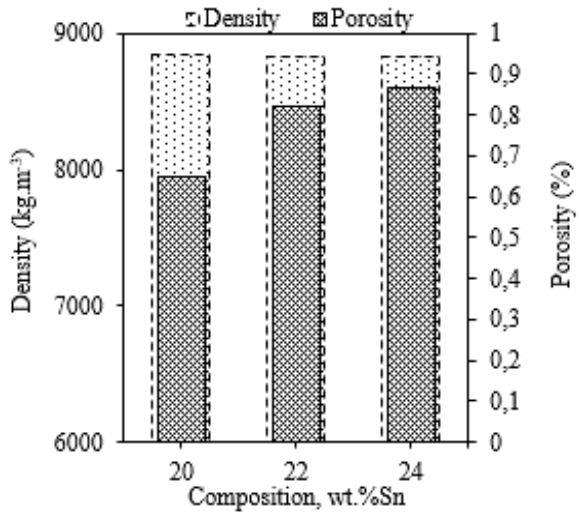

Fig. 8. Density and porosity

3.3. Mechanical properties

Mechanical properties including tensile strength and bending strength are affected by the homogeneity of the material structure. Tin bronze alloys through the sand casting method have low homogeneity. This is due to the rapid cooling rate avoiding the atoms in the alloy adjusting their position to form regular and homogeneous grains. Each structure of the material has a grain microstructure, diverse sizes, and shapes of porosity. Figure 9 shows the relationship between tensile strength and modulus of elasticity of Cu(20-24)wt% Sn which decreases with increasing tin composition. Tin bronze alloys become brittle with increasing tin composition.

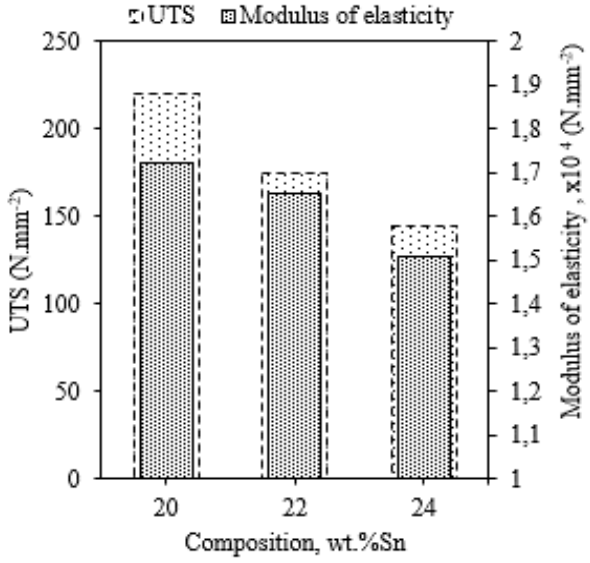

Fig. 9. Ultimate tensile strength and modulus of elasticity

Enhancing the tin composition in the tin bronze alloy through the sand casting method affects the mechanical properties. Copper metal has ductile properties while the tin metal trend to be brittle. The deflating copper composition while increasing tin alloy composition of Cu(20-24) wt.% Sn affect the modulus of elasticity of tin bronze alloy to decrease. The increase in porosity in Cu(20-24)wt.%Sn alloy also causes the tensile strength and modulus of elasticity of the tin bronze alloy to decrease. The ultimate tensile strength/ decreased from 219.51 $N.mm^{-2}$ to 143.91 $N.mm^{-2}$, the modulus of elasticity also decreased 12.2% (1.72 $x10^4$ $N.mm^{-2}$ to $1.51x10^4$ N.mm). The modulus of elasticity is a measure of the stiffness of a material, thus the higher the modulus of elasticity of a material, the smaller the change in shape that occurs in the material when given a force. The greater the modulus of elasticity, the smaller the elastic strain that occurs, and the stiffness of the material increases.

The bending strength decreases by 34.85% (533.95 $N.mm^{-2}$ to 395.95 $N.mm^{-2}$), while the hardness of the alloy increased by 23.86% (305.77 VHN to 378.73 VHN). The bending strength and hardness of Cu(20-24) wt% Sn are shown in Figure 10. The increase in hardness causes the tin bronze alloy Cu(20-24)wt.% Sn to become more brittle.

The increase in the hardness of the alloy metal is influenced by the magnitude of the solidification rate in the recrystallization zone [23]. The increased tin composition in the tin bronze alloy causes the solidification rate to decrease. It prolongs the time of the particles between the two elements in the alloy to diffuse and recrystallize. Changes in microstructure from coarse grains to fine columnar dendrite grains and increased segregation increases the hardness of the alloy metal[18]. Increased hardness is also impacted by reduced microporosity in the specimen[21]. Enhancing tin composition in the tin bronze alloy Cu(20-24)wt.%Sn lowers the mechanical properties of tensile strength and bending strength, but the hardness increases.

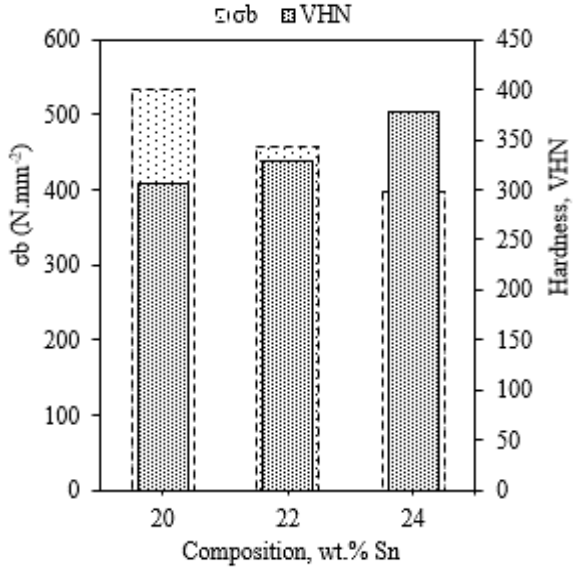

Fig. 10. Bending strength and hardness

3.4. Acoustical properties

The tin composition of 24wt.%Sn has a lower density and modulus of elasticity than 20wt.% Sn and 22wt.%Sn. The density and modulus of elasticity are the main parameters in determining the acoustic properties of metallic materials. The main parameters of acoustic properties including the speed of sound (c), impedance (z), and radiation coefficient (R) are strongly influenced by the density and modulus of elasticity. Table 2 shows the density, modulus of elasticity, and acoustic properties parameters of tin bronze alloys Cu(20-24)wt.% Sn by sand casting method.

The high density and modulus of elasticity in tin bronze alloys increase the speed of sound, impedance, and radiation coefficient. Tin bronze alloy Cu20wt.% Sn has acoustic parameters including speed of sound, impedance, and radiation coefficient higher than Cu22wt.% Sn and Cu24wt.% Sn. Metallic materials that have a low damping capacity release mechanical energy more slowly thus they can vibrate longer. The natural frequency spectrum and amplitude are influenced by the composition of the alloy, mechanical properties, and dimensions of musical instruments [24].

The damping capacity of several tin bronze alloy compositions is shown in Figure 11. The correlation results between Table 2 and Figure 11 shows that tin bronze alloy Cu20wt.% Sn produces higher sound intensity (dB) with low damping capacity. Tin bronze alloy Cu20wt.% Sn has damping capacity $y = 44.395e^{-512.9x}$. The damping capacity of tin bronze alloy Cu22wt.% Sn is $y = 38.013e^{-589.5x}$ and tin bronze alloy Cu24wt.% Sn is $y = 41.657e^{-1087x}$. The sound intensity (dB) of the Cu20wt.% Sn tin bronze alloy is higher at 40-50dB, while the Cu22wt.% Sn and Cu24wt.% Sn tin bronze alloys are lower at 30-40dB. Increased damping capacity occurs due to a decrease in physical and mechanical properties. The main copper matrix (Cu) in the tin bronze alloy serves to maintain plasticity so that stress and strain in the material increase. The damping capacity of cast iron increases with decreasing mechanical strength[14]. Tin bronze alloy Cu20wt.% Sn showed a higher sound intensity (dB) than alloy Cu22wt.% Sn and Cu24wt.% Sn.

Table 2.
Calculation of acoustic properties parameters of Cu bronze alloy (20-24) wt% Sn [13]

Alloys	(ρ) kg.m^{-3}	(E) kg.m^{-2}	Speed of sound (c) m.det^{-1}	Impedance (z) kg.m^{-2}.det^{-1}	Radiation coefficient (R) m^{4}.kg^{-1}.det^{-1}
Cu20wt.%Sn	8.842E+03	1.69E+09	436.903	3.86E+06	4.96E-02
Cu22wt.%Sn	8.826E+03	1.68E+09	436.708	3.85E+06	4.95E-02
Cu24wt.%Sn	8.822E+03	1.54E+09	417.236	3.68E+06	4.73E-02

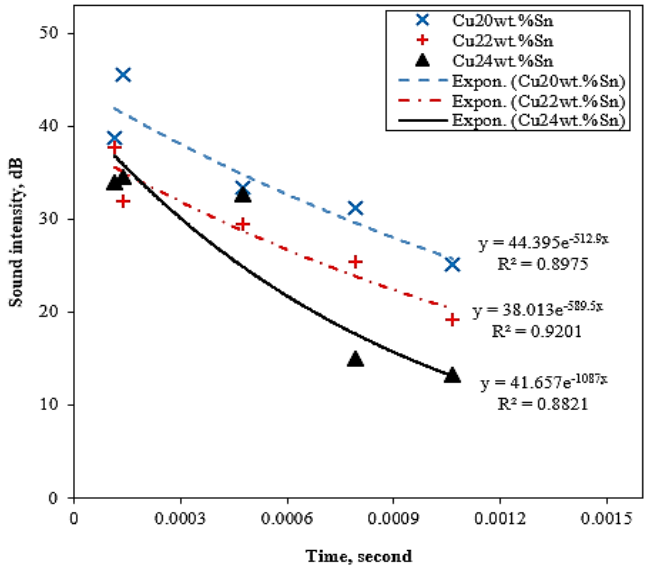

Fig. 11. The damping capacity of tin bronze Cu(20-24)wt.%Sn

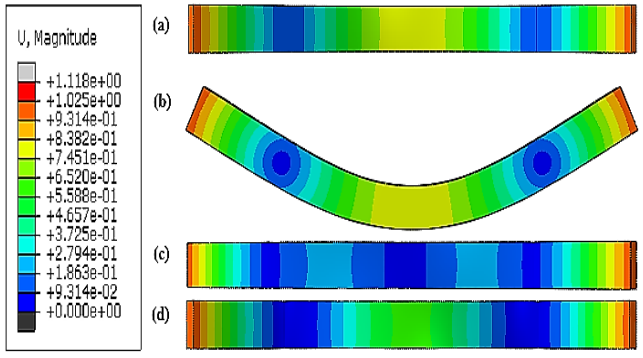

Fig. 12. Vibration modes shape of the specimen rod (a) mode 1 (b) mode 2 (c) mode 3 (d) mode 4

The vibrations that occur in the specimen rod (ASTM E1876-01) cause a displacement as proven by the finite element analysis (FEA) simulation of tin bronze alloys shown in Figure 12. The stress acting on the specimen rod causes a maximum displacement of 1.118 mm. Figure 12 shows the natural frequency of the experimental method of analysis (EMA) tin bronze alloy Cu(20-24)wt.%Sn. The natural frequency of tin bronze alloys decreases with increasing tin composition. Tin composition Cu20wt.%Sn has a higher natural frequency followed by Cu22wt.%Sn and Cu24wt.%Sn.

Table 3 shows the natural frequencies of each shape for the tin bronze alloy Cu(20-24) wt.% Sn between FEA and EMA. Cu20wt.% Sn tin bronze shows a higher natural frequency than other tin bronze. The increase in the tin bronze composition of Cu (20-24)wt.% Sn causes a decrease in natural frequency. Tin bronze alloy Cu20wt.% Sn produces a higher natural frequency, FEA = 14807.0 Hz and EMA = 14986.0 with an absolute error rate of 1.19. The natural frequency of tin bronze alloy Cu22wt.% Sn has FEA = 12111.0 and EMA = 12842.0 with an absolute error of 5.69 and Cu24wt.% Sn have FEA = 12079.0 and EMA = 11683.0 with an absolute error of 3.39. The increased natural frequency means that the specimen can produce sound when the specimen is hit.

The mechanical properties of the modulus of elasticity affect the stiffness of the material. The stiffness brighter of the material (k) is proportional to the magnitude of the modulus of elasticity (E). The mechanical property of stiffness is the main variable in determining the sound wavelength (ωn). The sound wavelength (ωn) is the root product of the mechanical properties of stiffness (k) divided by the mass (m), shown in Equation (8).

$$\omega_n = \sqrt{k/m} \tag{8}$$

Natural frequency analysis through the experimental method analysis/ EMA on the tin bronze alloy Cu20wt.% Sn results in the highest higher natural frequency of 14986 Hz. While Cu22wt.% Sn and Cu24wt.% Sn result 12842 Hz and 11683 Hz respectively. The increments of natural frequency improvement are 27.60%, 36.85%, and 48.87% respectively to Cu20wt.% Sn, Cu22wt.% Sn and Cu24wt.% Sn. The natural frequency of tin bronze analyzed by finite element analysis (FEA) exhibits 14807.0 Hz, 12111.0 Hz, and 12079.0 Hz for Cu20wt.% Sn, Cu22wt.% Sn, Cu24wt.% Sn respectively. The improvement of natural frequency is 26.84%, 37.71%, and 51.59% for Cu20wt.% Sn, Cu22wt.% Sn and Cu24wt.% Sn respectively. The absolute error of the highest natural frequency between FEA and EMA on the tin bronze alloy is 13.23%, 10.87%, and 14.45% respectively to Cu20wt.% Sn, Cu22wt.% Sn and Cu24wt.% Sn. The tin bronze alloy Cu20wt.% Sn through FEA and EMA methods exhibit the highest natural frequency.

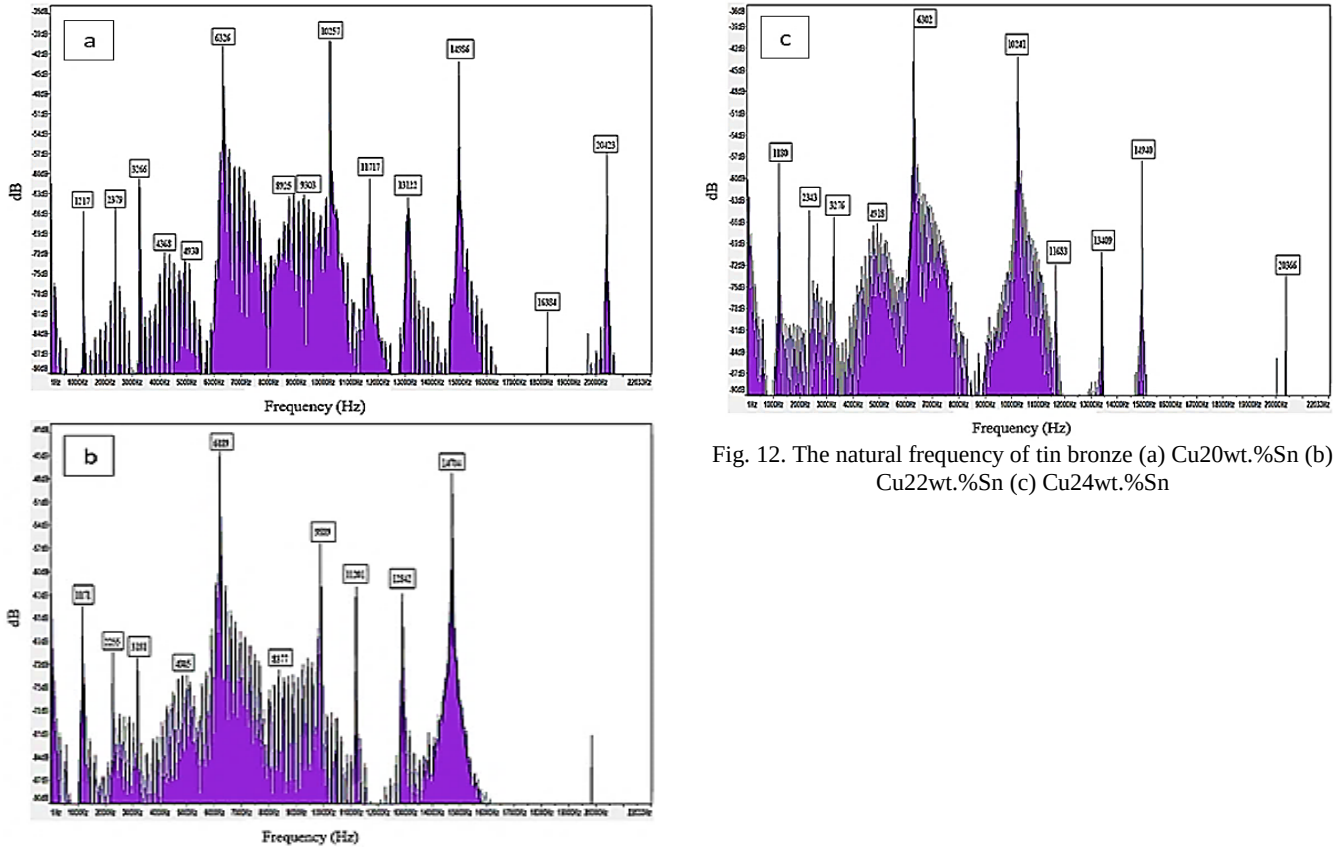

Fig. 12. The natural frequency of tin bronze (a) Cu20wt.%Sn (b) Cu22wt.%Sn (c) Cu24wt.%Sn

Table 3.
The natural frequency of each mode shapes for the tin bronze alloy Cu(20-24)wt% Sn between FEA and EMA.

Alloys	Natural frequencies (Hz)	Mode shapes											
		1	2	3	4	5	6	7	8	9	10	11	12
Cu20wt.%Sn	FEA	1293.6	2457.2	3587.4	3822.7	5582.0	6643.9	8379.0	8379.4	10120.0	11703.0	12620.0	14807.0
	EMA	1217.0	2379.0	3266.0	4368.0	4930.0	6326.0	8925.0	9303.0	10257.0	11717.0	13122.0	14986.0
	Absolute error(%)	6.29	3.29	9.84	12.48	13.23	5.03	6.12	9.93	1.34	0.12	3.83	1.19
Cu22wt.%Sn	FEA	1058.1	2009.8	3126.7	4565.8	6040.2	8277.2	9572.4	10323.0	12111.0	-	-	-
	EMA	1171.0	2255.0	3181.0	4805.0	6189.0	8377.0	9889.0	11201.0	12842.0	-	-	-
	Absolute error(%)	9.64	10.87	1.71	4.98	2.40	1.19	3.20	7.84	5.69	-	-	-
Cu24wt.%Sn	FEA	1055.3	2004.5	3118.4	4553.6	6835.2	10295.0	12079.0	-	-	-	-	-
	EMA	1180.0	2343.0	3276.0	4918.0	6302.0	10241.0	11683.0	-	-	-	-	-
	Absolute error(%)	10.57	14.45	4.81	7.41	8.46	0.53	3.39	-	-	-	-	-

4. Conclusions

1. The enhancement of the tin composition of the tin bronze alloy Cu(20-24) wt.% Sn produced by the sand casting method has resulted in a microstructure with fine grains in the form of columnar dendrites. Physical properties analysis reveals a decreasing density that increasing porosity. Mechanical properties i.g tensile strength, modulus of

elasticity, and bending strength lowers, while the hardness of the tin bronze alloy increases.

2. The improvement of physical and mechanical properties increases the acoustic properties parameters i.g the speed of sound (c), impedance (z), and radiation coefficient (R). The superior acoustic properties are also characterized by a high natural frequency and low damping capacity, meaning that the tin bronze alloy is capable of producing high frequencies, short waves with longer vibration times. Upon the advantages of physical and mechanical properties, tin bronze alloy Cu20wt.% Sn is convinced recommended as raw material for producing gamelan musical instruments through the sand casting method.

Acknowledgment

The research was conducted under a dissertation grant by the Indonesian Ministry of Finance through Lembaga Pengelola Dana Pendidikan (LPDP) - BUDI DN scholarship program No. PRJ-6851 /LPDP.3/2016.

References

[1] Sumarsam. (2002). Introduction to Javanese gamelan (Javanese gamelan-beginners). Wesleyan University. Middletown.
[2] Sutton, R.A. (2007). Gamelan: The Traditional Sounds of Indonesia (review). *Asian Music*. 38(1), 142-144.
[3] Suyanto, Tjokronegoro H.A, Merthayasa I.G.N. & Supanggah R. (2015). Acoustic parameter for javanese gamelan performance in pendopo mangkunegaran Surakarta. *Procedia – Social and Behavioral Sciences.* 184. 322-327.
[4] Goodway, M. (1992). Metals of music. *Materials Characterization*. 29. 177-184.
[5] Audy, J. & Audy, K. (2008). Analysis of bell materials: Tin bronzes. *China Foundry*. 5(3). 199-204.
[6] Debut, V. Carvalho, M. Figueiredo, E. Antunes, J. & Silva, R. (2016). The sound of bronze: Virtual resurrection of a broken medieval bell. *Journal of Cultural Heritage*. 19. 544-554.
[7] Sugita, I.K.G. Soekrisno, R. Miasa, I.M. & Suyitno. (2011). Mechanical and damping properties of silicon bronze alloys for music applications. *International Journal of Engineering &. Technology*. 11(6). 81-85.
[8] Sugita, I.K.G. Soekrisno, R. & Miasa, I.M. (2011). The effect of annealing temperature on damping capacity of the bronze 20 % Sn alloy. *International Journal of Mechanical & Mechatronics Engineering*. IJMME-IJENS. 11(4).1-5.
[9] Slamet, S. Suyitno, & Kusumaningtyas, I. (2019). Effect of composition and pouring temperature of Cu (20-24) wt.% Sn by sand casting on fluidity and Mechanical Properties, *Journal of Mechanical Engineering and Science.* 13(4). 6022-6035.
[10] Sugita, I.K.G. & Miasa, I.M. (2013). Feasibility Study On The Use Of Silicon-Bronze Alloys As An Alternative Material For Balinese Musical Instruments. *20th International Congress on Sound & Vibration*; 7-11 July 2013.1-5. Bangkok, Thailand
[11] Prayoga, B.T. Suyitno, Dharmastiti, R. & Akbar, F. (2018). Microstructural characterization, defect, and hardness of titanium femoral knee joint produced using vertical centrifugal investment casting. *Journal of Mechanical Science and Technology.*32(1).149-156.
[12] Salonitis, K. Jolly, M. & Zeng, B. (2017). Simulation-based energy and resource-efficient casting process chain selection : A case study. *Procedia Manufacturing.* 8. 67-74.
[13] Wegst, U.G. (2006). Wood For Sound. *American Journal of Botany*. 93.1439-1448.
[14] Adams, R. D. & Fox, M.A.O. (1973). Correlation of the damping capacity of cast iron with its mechanical properties and microstructure. *Journal of Mechanical Engineering Science.* 15(2). 81-94.
[15] Grafov, B.M. (1994). The archimedes law and electrocapillarity. *Electrochimica Acta*. 39. 467-469.
[16] ASTM. (2015). Standard test methods for bend testing of material for ductility.1.1-10.
[17] Sutiyoko & Suyitno. (2012). Effect of pouring temperature and casting thickness on fluidity, porosity and surface roughness in lost foam casting of gray cast iron. *Procedia Engineering*. 50. 88-94.
[18] Halvaee, A. & Talebi, A. (2001). Effect of process variables on microstructure and segregation in the centrifugal casting of C92200 alloy. *Journal of Materials Processing Technology*. 118, 123-127.
[19] Sutiyoko. Suyitno. & Mahardika. M. (2016). Effect of gating system on porosity and surface roughness of femoral stem in centrifugal casting. *Adv. Sci. Technol. Soc. AIP Conference Proceedings*. 1755, 1-6.
[20] Sulaiman, S. & Hamouda, A.M.S. (2004). Modeling and experimental investigation of the solidification process in sand casting. *Journal of Materials Processing Technology*. 156, 1723-1726.
[21] Nadolski, M. (2017). The Evaluation of Mechanical Properties of High-tin Bronzes. *Archives of Foundry Engineering*. 17(1), 127-130.
[22] Nimbulkar, S.L. & Dalu. R.S. (2016). Design optimization of gating and feeding system through simulation technique for sand casting of wear plate. *Perspectives in Science*. 8.39-42.
[23] Singh, R. & Singh, S. (2013). Effect of process parameters on surface hardness, dimensional accuracy, and surface roughness of investment cast components; *Journal of Mechanical Science and Technology*. 27(1), 191-197.
[24] Bartocha, D. & Baron, C. (2016). Influence of tin-bronze melting and pouring parameters on its properties and bells ' tone. *Archives of Foundry Engineering*. 16(4), 17-22.